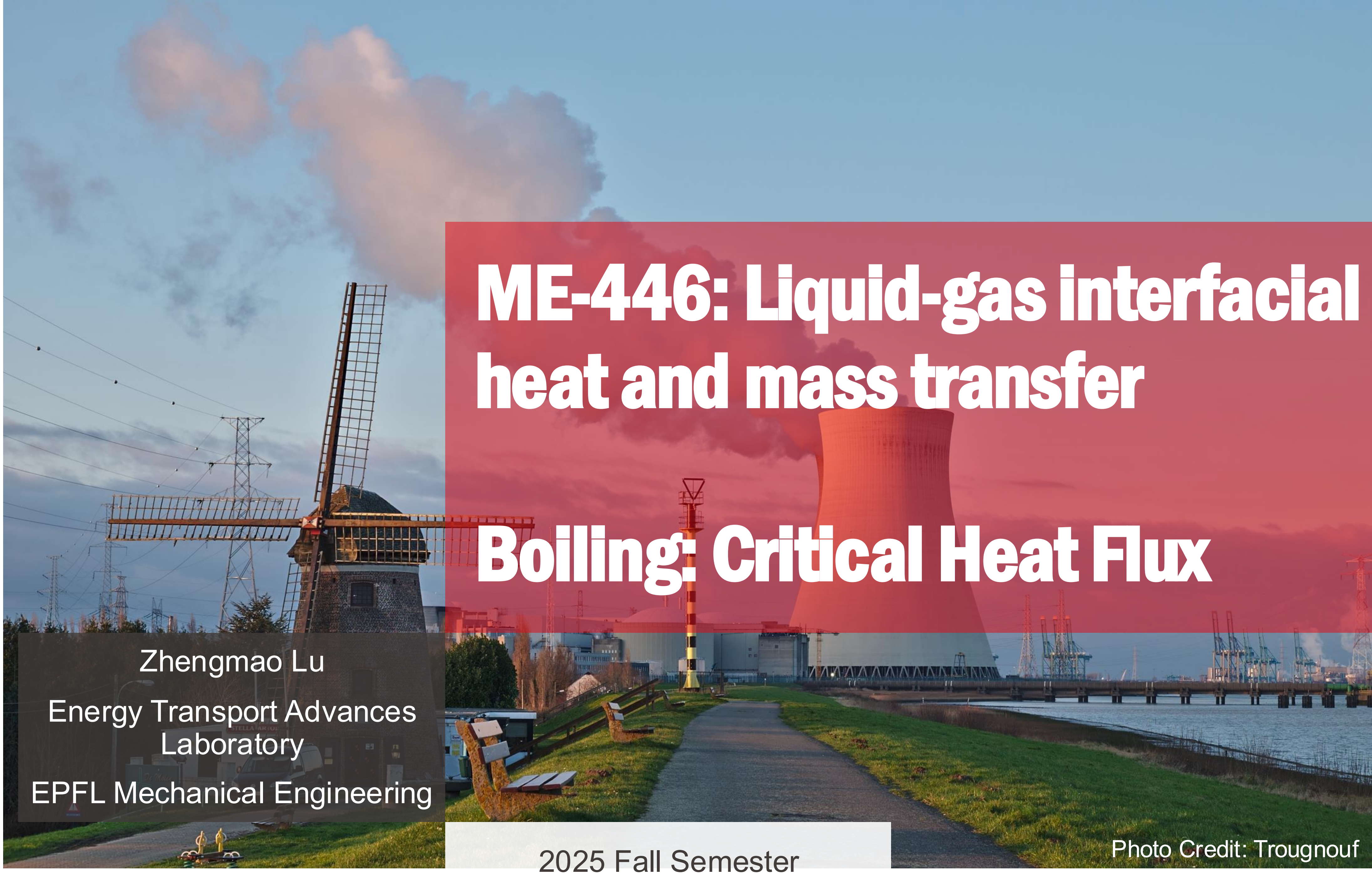

ME-446: Liquid-gas interfacial heat and mass transfer

Boiling: Critical Heat Flux

Zhengmao Lu

Energy Transport Advances Laboratory

EPFL Mechanical Engineering

2025 Fall Semester

Photo Credit: Trougnouf

Last Time

- Pool boiling curve
- Rohsenow’s microconvection model for nucleate boiling
- Helmholtz and Taylor instabilities

Pool Boiling Curve

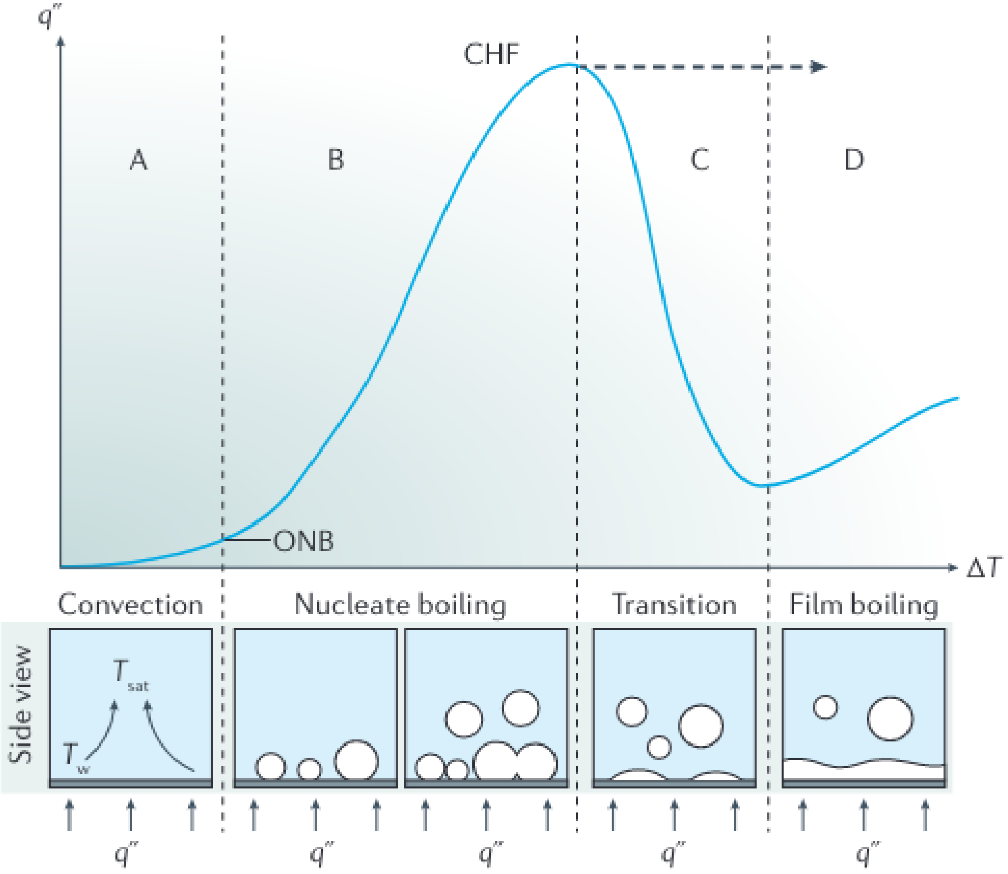

A. At very low superheats, heat transfer is mostly due to natural convection

B. After superheat is large enough to form vapor bubbles, nucleate boiling dominates, promoting bubble-motion-induced convection

C-D. After vapor generation becomes too much, passing the critical heat flux (CHF), insulating vapor film will start to form, decreasing the HTC

Rohsenow's Microconvection Model

Convective transport facilitated by bubbles

$$\mathrm{Nu}_b = \frac{hL_b}{k_l} \propto \mathrm{Re}_b^{1-r}\mathrm{Pr}_l^{1-s}$$

$$\mathrm{R}e_b = \frac{\rho_v U L_b}{\mu_L} \qquad U = \frac{q''}{\rho_v h_{lv}} = \frac{h\Delta T}{\rho_v h_{lv}}$$

$$\frac{q''}{\mu_l h_{lv}}\left[\frac{\sigma}{g(\rho_l - \rho_v)}\right]^{1/2} = \left(\frac{1}{C_{sf}}\right)^{1/r} \mathrm{Pr}_l^{-s/r}\left[\frac{c_{pl}\Delta T}{h_{lv}}\right]^{1/r}$$

Helmholtz Instability

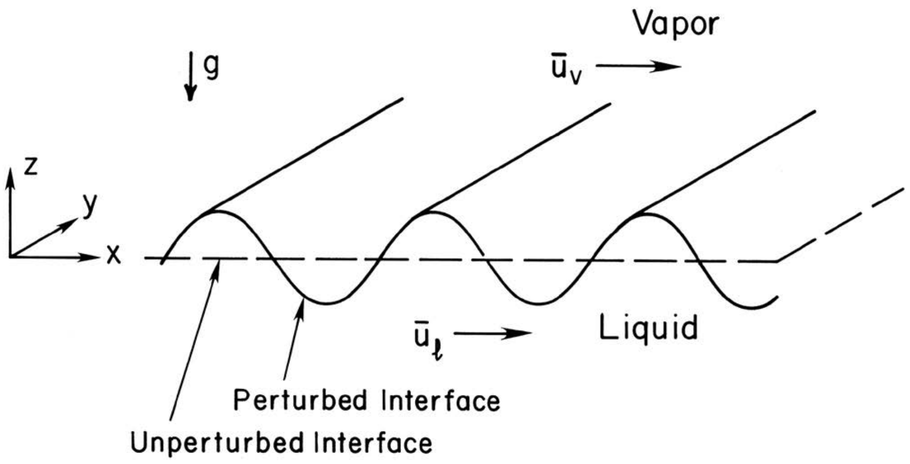

Perturbation $\delta(x, t = 0) = Ae^{i\alpha x}$

Response: $\delta = Ae^{i\alpha x + \beta t}$

$$\beta = \pm \frac{\sqrt{\alpha^2 \rho_v \rho_l (\bar{u}_v - \bar{u}_l)^2 - (\sigma \alpha^3 + \Delta\rho g \alpha)}}{\rho_v + \rho_l} - i\alpha \frac{\rho_l \bar{u}_l + \rho_v \bar{u}_v}{\rho_v + \rho_l}$$

- Instability condition: $|\bar{u}_v - \bar{u}_l| > \sqrt{\frac{\left(\sigma\alpha + \frac{\Delta\rho g}{\alpha}\right)(\rho_l + \rho_v)}{\rho_l \rho_v}}$
- When $|\bar{u}_v - \bar{u}_l| > \left[\frac{2(\rho_l + \rho_v)}{\rho_l}\right]^{\frac{1}{2}} \left(\frac{\sigma \Delta\rho g}{\rho_v^2}\right)^{\frac{1}{4}}$, there will be some wave number α growing exponentially
- $\bar{u}_v - \bar{u}_l$ promotes instability while gravity and surface tension suppressing instability, we can adjust the value of g based on the orientation of the system.

Vapor Column Instability

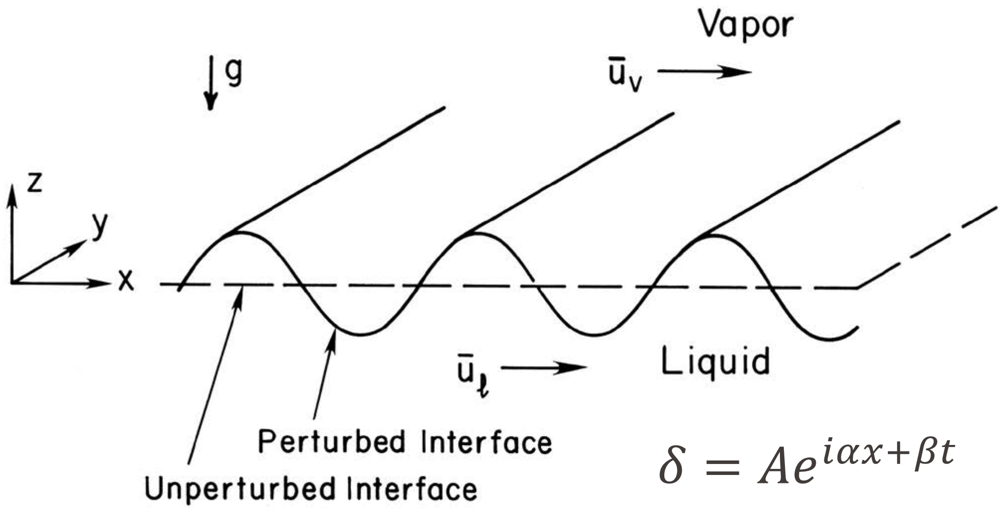

$$\delta = Ae^{i\alpha x+\beta t}$$

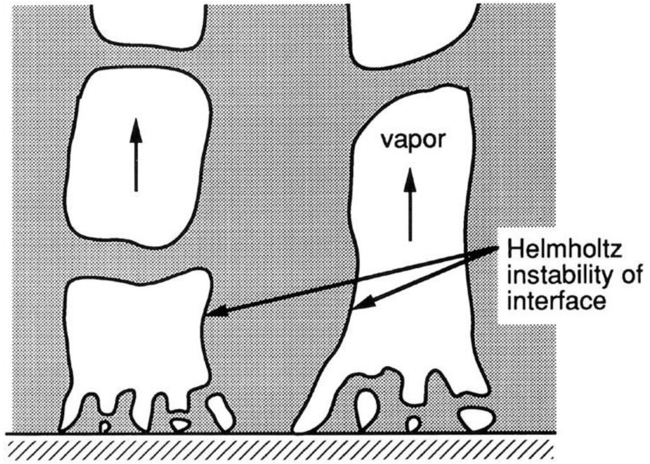

Setting g = 0 for in Helmholtz instability for vertical surfaces

$$|\bar{u}_v - \bar{u}_l| > \sqrt{\frac{\sigma\alpha\,(\rho_l + \rho_v)}{\rho_l\rho_v}} = \sqrt{\frac{2\pi\sigma\,(\rho_l + \rho_v)}{\rho_l\rho_v\lambda_H}}$$

Taylor Instability

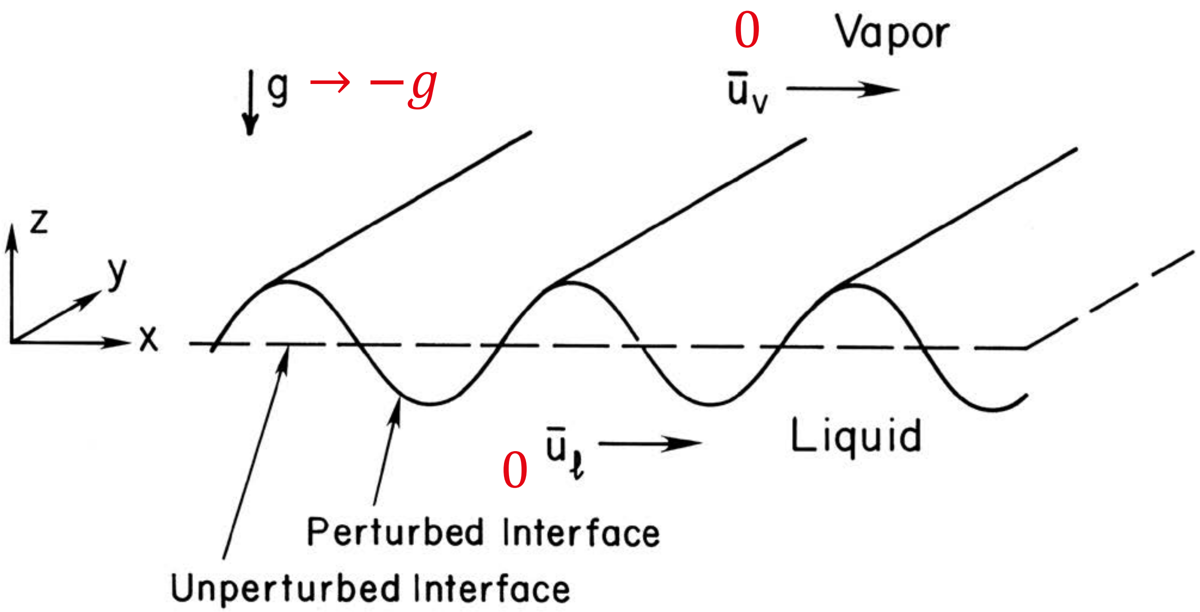

Liquid on top of vapor

$$\delta = Ae^{i\alpha x+\beta t}$$

$$\beta = \pm\sqrt{\frac{\Delta\rho g\alpha - \sigma\alpha^3}{\rho_l + \rho_v}}$$

The fastest growing perturbation (α_{max}) in this case can be found by setting $\frac{d\beta}{d\alpha} = 0$

The corresponding most dangerous wavelength $\lambda_D = \frac{2\pi}{\alpha_{max}} = 2\pi\sqrt{\frac{3\sigma}{\Delta\rho g}}$

ILOs Today

- Zuber’ CHF model based on hydrodynamic instability
- Force balance model for CHF
- Statistical approach for CHF

Zuber's Model Assumptions

$$|\bar{u}_v - \bar{u}_l| > \sqrt{\frac{\sigma\alpha\,(\rho_l + \rho_v)}{\rho_l \rho_v}} = \sqrt{\frac{2\pi\sigma\,(\rho_l + \rho_v)}{\rho_l \rho_v \lambda_H}}$$

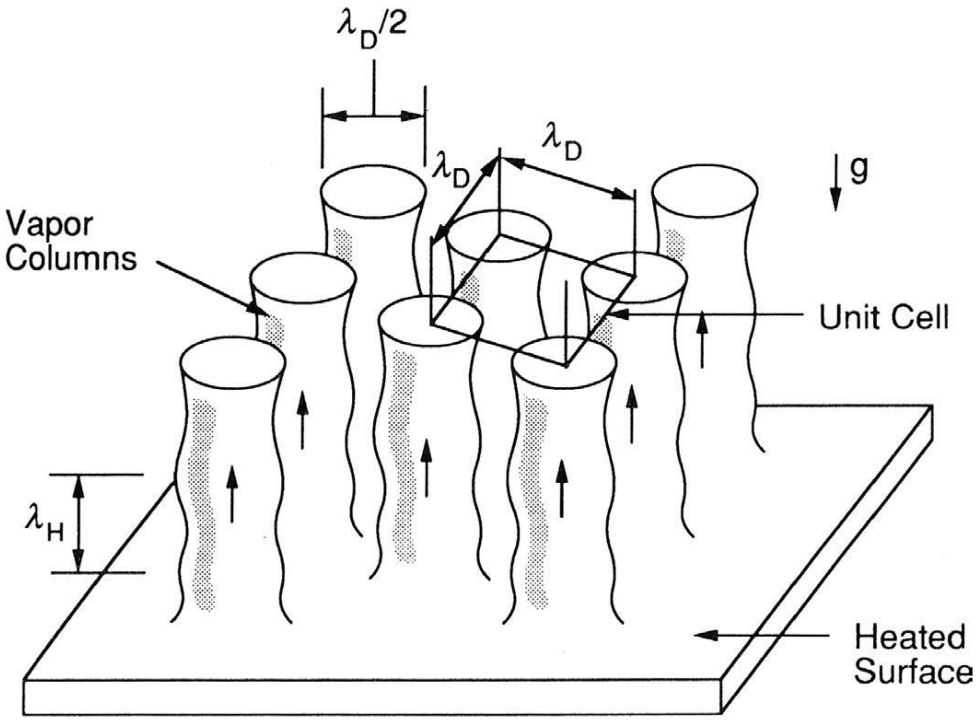

- Vapor columns are formed near CHF
- CHF is reached when interface of vapor columns becomes Helmholtz unstable (λ_H)
- The pitch of the vapor columns coincides with the most dangerous wavelength in Taylor instability

$$\lambda_D = 2\pi\sqrt{3\sigma/\Delta\rho g}$$

- The diameter of vapor column is $\lambda_D/2$
- Assuming $\lambda_H = \lambda_D \Rightarrow u_c = \sqrt{\frac{2\pi\sigma\,(\rho_l+\rho_v)}{\rho_l \rho_v \lambda_H}} \approx \sqrt{\frac{2\pi\sigma}{\rho_v \lambda_D}}$

Zuber's CHF Prediction

$$u_c = \sqrt{\frac{2\pi\sigma}{\rho_v \lambda_D}} \qquad \lambda_H = \lambda_D = 2\pi\sqrt{\frac{3\sigma}{\Delta\rho g}}$$

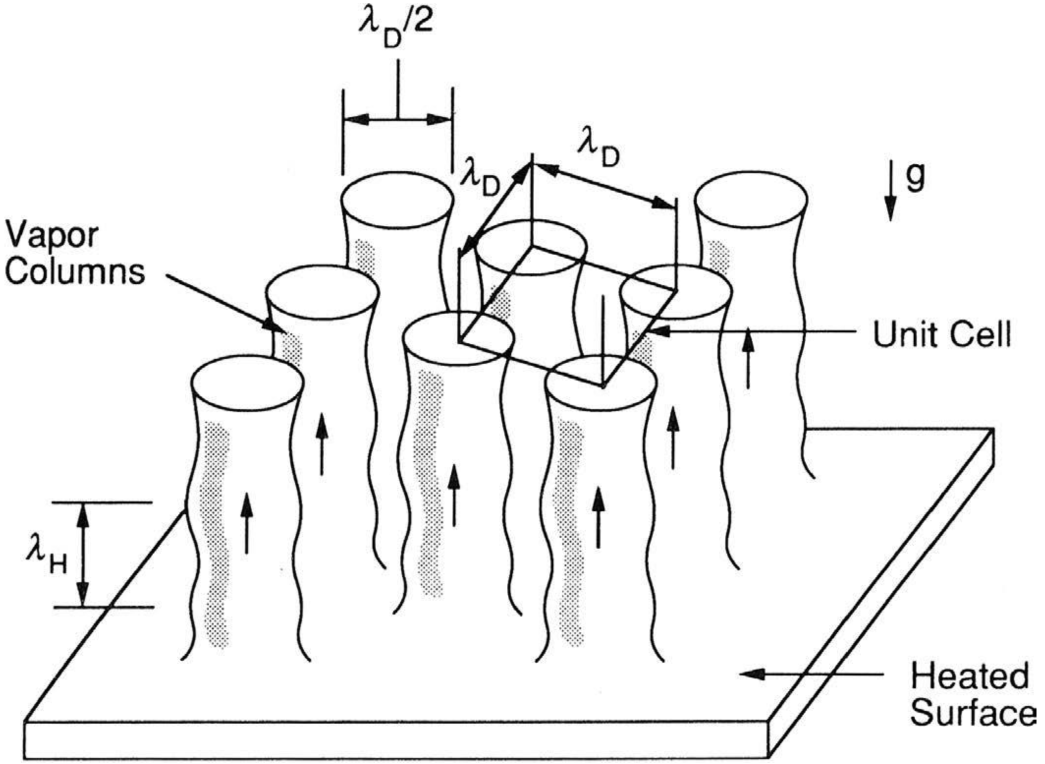

$$u_c = \frac{q''_{max}}{\rho_v h_{lv}}\left(\frac{A_{surf}}{A_{col}}\right) = \frac{16}{\pi}\frac{q''_{max}}{\rho_v h_{lv}}$$

$$q''_{max} = 0.149\rho_v h_{lv}\left(\frac{\sigma\Delta\rho g}{\rho_v^2}\right)^{1/4}$$

Comments on Zuber’s Model

- No way to accommodate effects from geometry and surface wettability
- No clear justification for the choice of vapor column diameter as $\lambda_D/2$
- No visual observation of Helmholtz instability during boiling to date
- Still widely used as a reference model for all subsequent CHF models

Lateral Force Balance Model

Kandlikar 2001 https://doi.org/10.1115/1.1409265

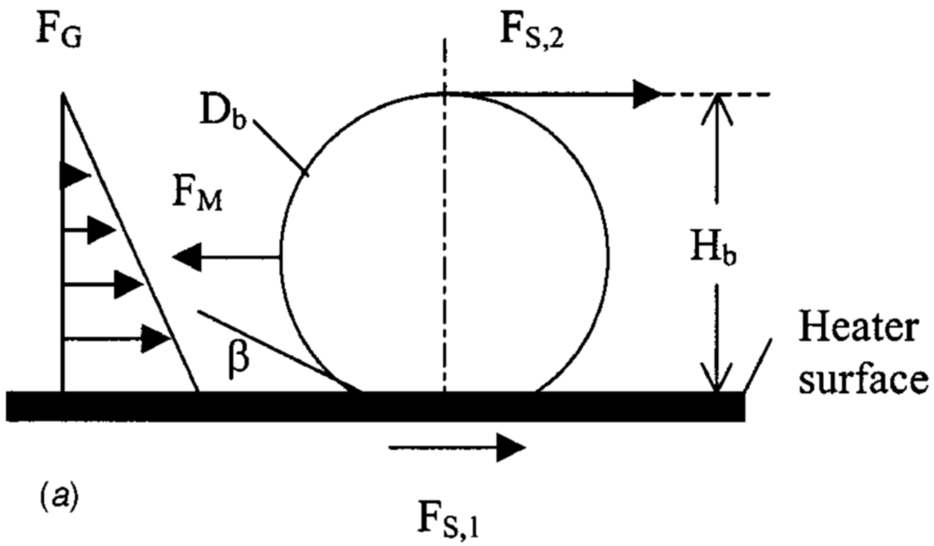

Considering the lateral direction on half of a bubble

Surface tension force : $F_{s,1}$, $F_{s,2}$

Hydrostatic force: F_G

Momentum force: F_M (due to phase change)

Simple force balance requires $F_{s,1} + F_{s,2} + F_G = F_M$

Choose a bubble diameter at CHF $D_b = \lambda_D/2$

λ_D: the most dangerous wavelength in Taylor instability $\lambda_D = 2\pi\sqrt{\frac{3\sigma}{\Delta\rho g}}$

and set a bubble influence area πD_b^2

Contact Angle Dependence

$$q''_K = \rho_v h_{fg}\left(\frac{1+\cos\beta}{16}\right)\left[\frac{2}{\pi}+\frac{\pi}{4}(1+\cos\beta)\right]^{\frac{1}{2}}\left(\frac{\sigma\Delta\rho g}{\rho_v^2}\right)^{1/4}$$

(Horizontal surface)

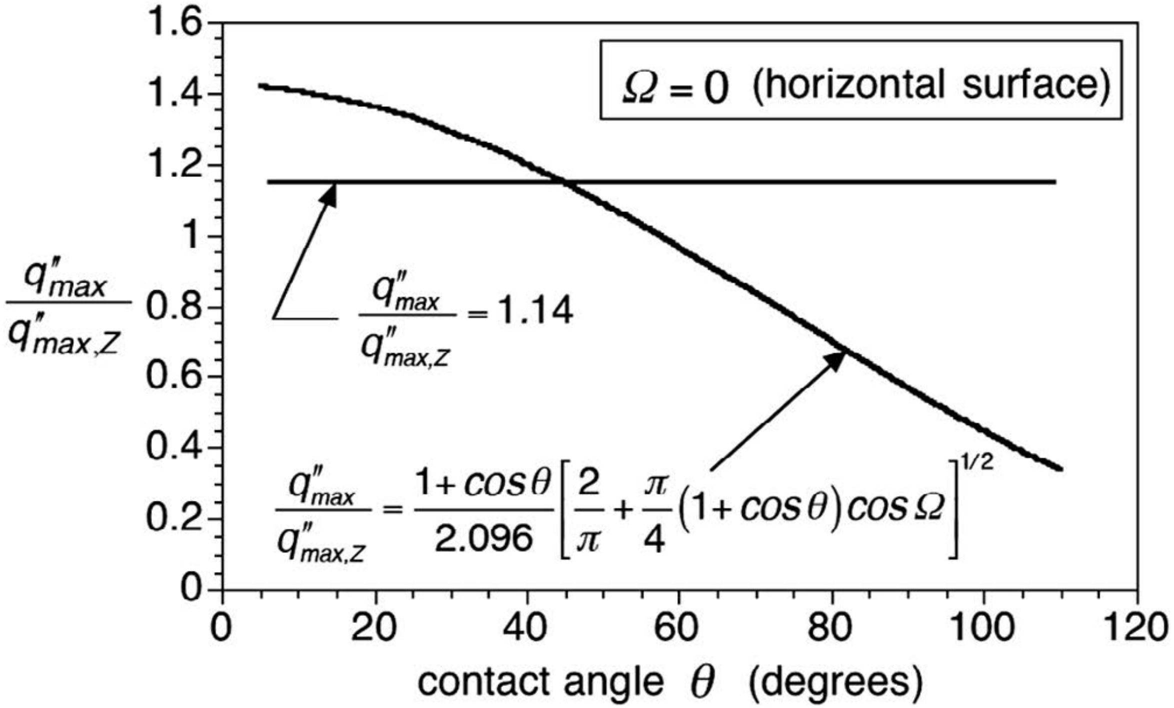

FIGURE 7.19 in Carey

$$q''_{max,Z} = 0.149\rho_v h_{lv}\left(\frac{\sigma\Delta\rho g}{\rho_v^2}\right)^{1/4}$$

$$\frac{q''_K}{q''_{max,Z}} = \frac{1+\cos\theta}{2.096}\left[\frac{2}{\pi}+\frac{\pi}{4}(1+\cos\beta)\right]^{\frac{1}{2}}$$

Comments on Kandlikar's Model

Dhillon *et al.*, *Nat Commun* 2015

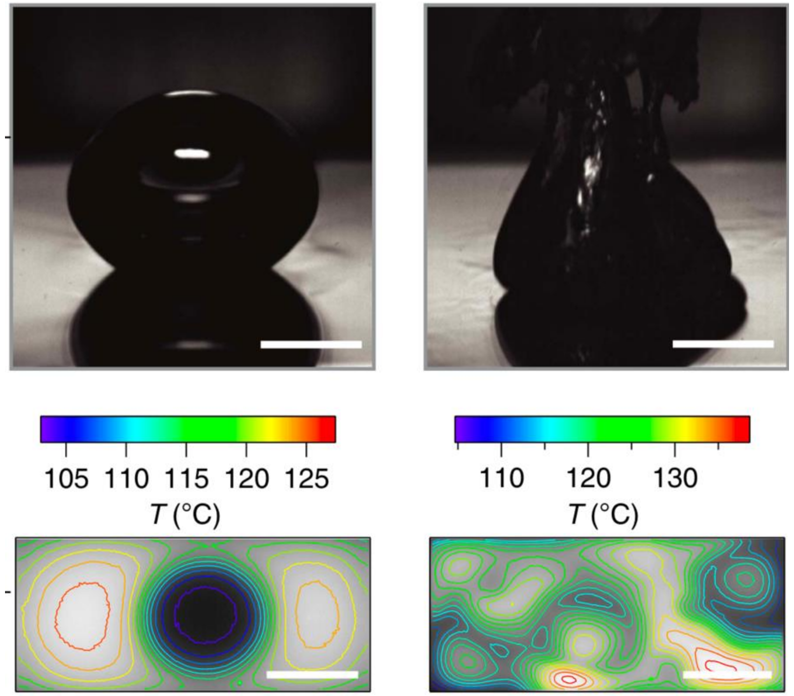

Choice of geometric parameters not quite justified at CHF

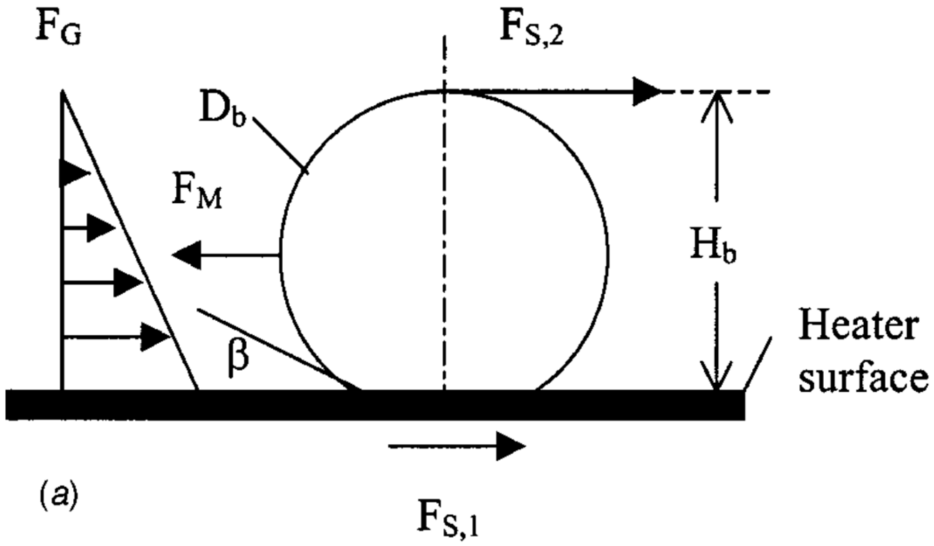

$$F_{s,1} + F_{s,2} + F_G = F_M$$

Liquid-vapor pressure difference not accounted for in momentum balance

Statistical Approach for Flat Surface Boiling

Working fluid: R134a

Heat flux:
from 1.5 W/cm^2 to 38 W/cm^2

Yazdani, 2016
https://doi.org/10.1063/1.4940042

Population Distribution of Nucleation Sites

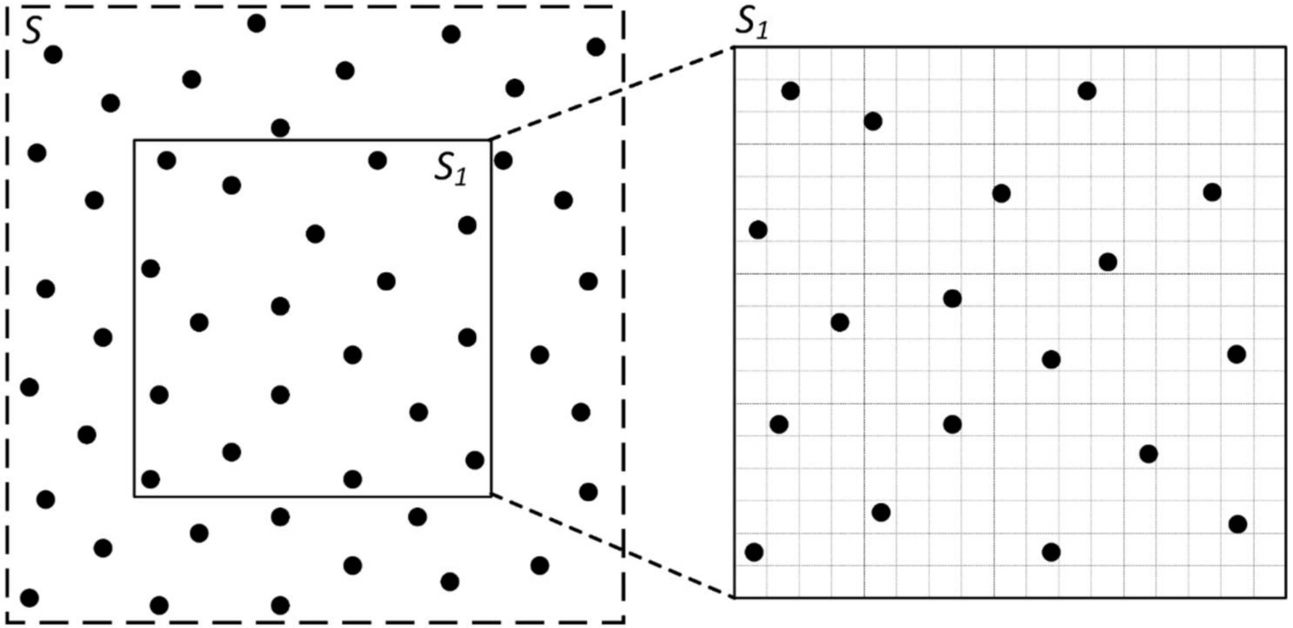

https://doi.org/10.1016/j.ijheatmasstransfer.2021.121904

- Consider a large surface S (large enough to ignore edge effects)
- Assume that probability of each point on the surface becoming an active nucleation sites is equal

Population Distribution of Intrinsic Nucleation Sites

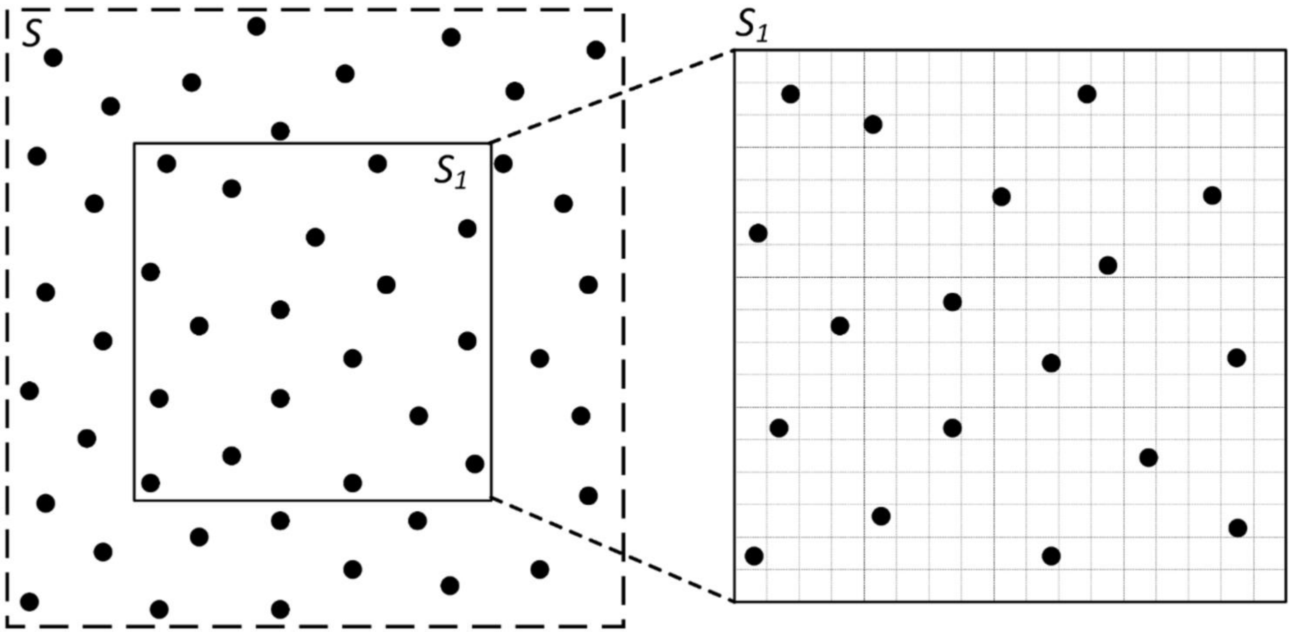

- The actual number of active nucleation sites in S_1, ***N***, can be considered as a random variable with an expectation value N_0
- Average nucleation density n_0 [m^{-2}], can be defined as $n_0 = N_0/A$
- n_0 can be assumed as a surface property

Population Distribution of Intrinsic Nucleation Sites

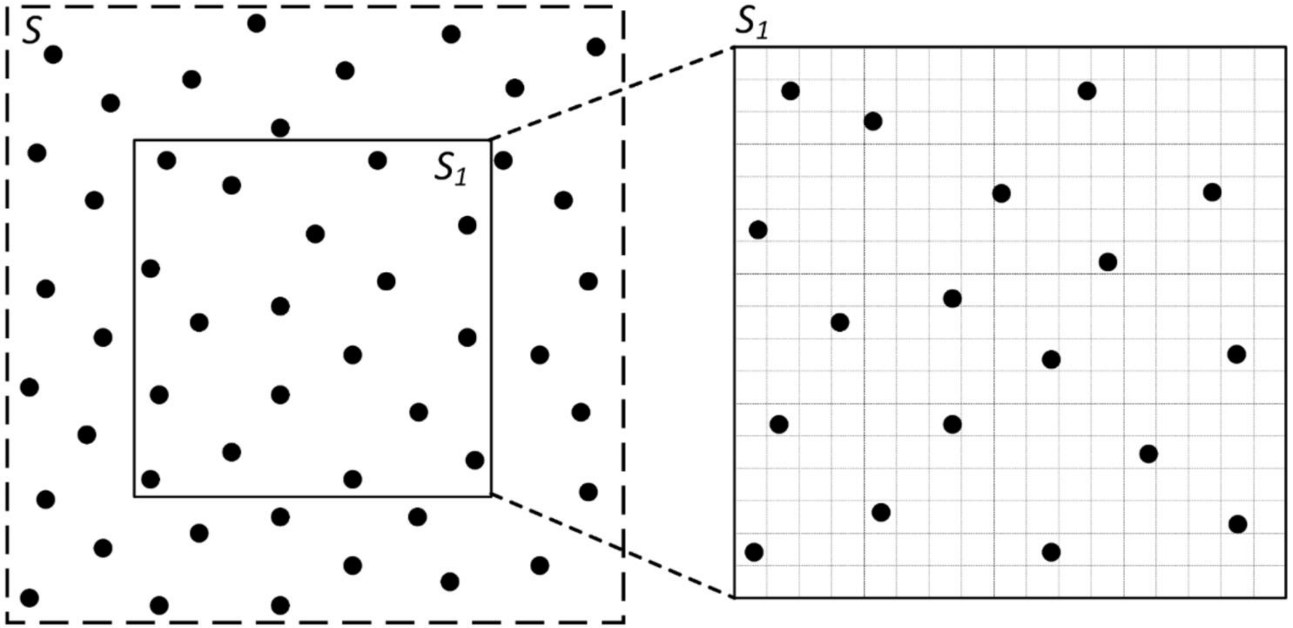

- Divide S_1 into *M* segments, each with the same area *A/M*
- Make *M* large enough such that the number of nucleation sites in each square is 0 or 1.
- Probability of finding a nucleation site in each square $p=N_0/M$

Population Distribution of Intrinsic Nucleation Sites

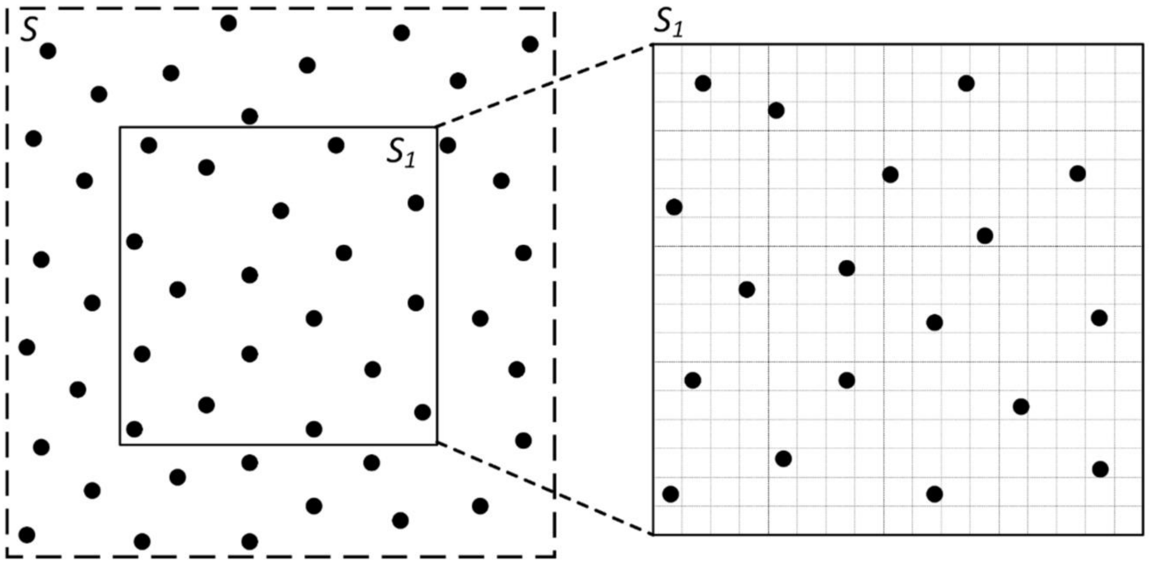

$$P(N, N_0, M) = \frac{1}{N!} \cdot \frac{M!}{(M-N)!\,M^N} \cdot N_0^N \left(1 - \frac{N_0}{M}\right)^{M-N}$$

Stirling's approximation: $\ln(n!) = n \ln n - n + O(\ln n)$ for $n \rightarrow \infty$

$$\lim_{M\to\infty} \ln\left[\frac{M!}{(M-N)!\,M^N}\right] = 0 \Rightarrow \lim_{M\to\infty} \frac{M!}{(M-N)!\,M^N} = 1$$

$$\lim_{M\to\infty} P(N, N_0, M) = \frac{N_0^N}{N!} e^{-N_0}$$

Population Distribution of Intrinsic Nucleation Sites

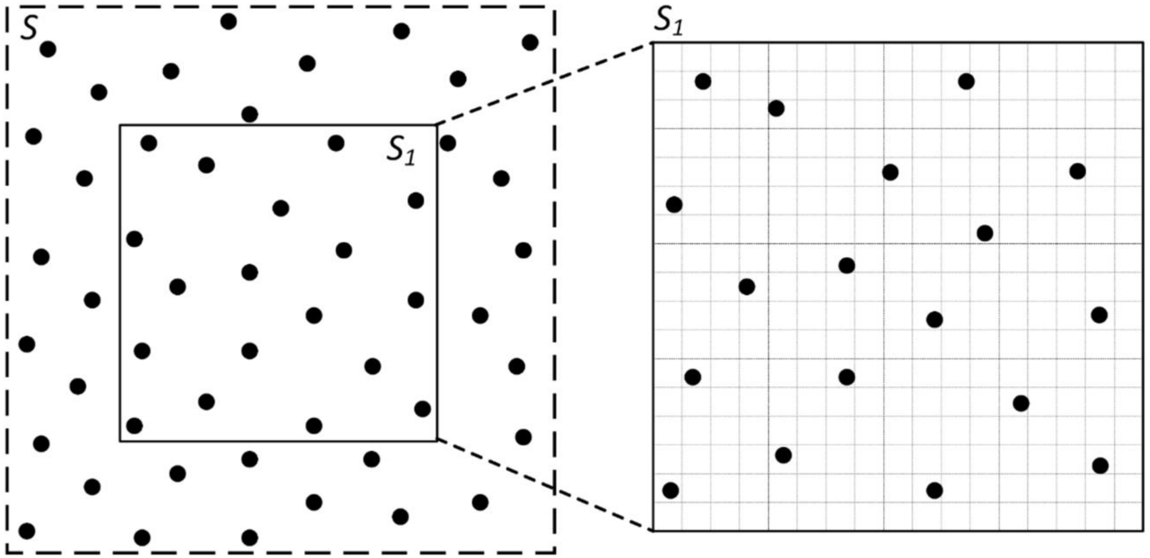

- Probability of finding N squares that contain one nucleation site is a binomial distribution

$$P = \frac{M!}{N!\,(M-N)!}p^N(1-p)^{M-N} = \frac{1}{N!}\cdot\frac{M!}{(M-N)!\,M^N}\cdot N_0^N\left(1-\frac{N_0}{M}\right)^{M-N}$$

Poisson Distribution

$$\mathrm{Po}(N, N_0) = \frac{N_0^N}{N!} e^{-N_0}$$

$$\sum_{N=0}^{\infty} P(N, N_0) = \sum_{N=0}^{\infty} \frac{N_0^N}{N!} e^{-N_0} = e^{N_0} \cdot e^{-N_0} = 1$$

What Marks the CHF

- Isolated bubbles dissipate heat better than merged bubbles
- CHF is reached when you have the **maximum number** of isolated bubbles
- With elevated temperature, 1) more nucleation sites become activated while 2) more bubbles are likely to merge into each other.

Nearest Neighbor (NN) Distance Between Nucleation Sites

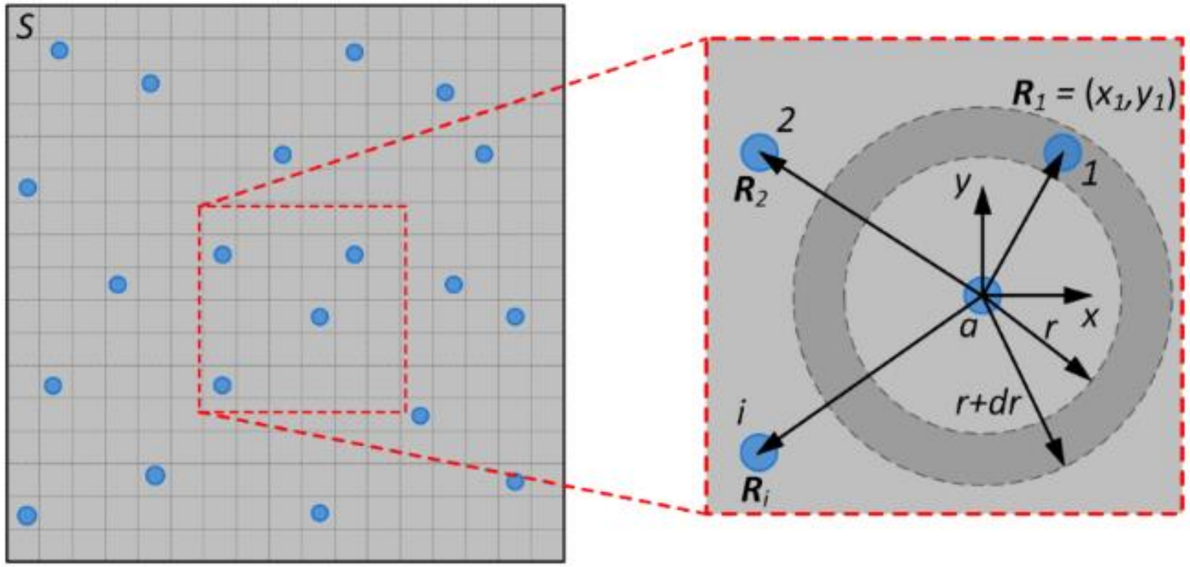

- We would like to know the probability distribution function for distance between two nearest activated nucleation sites

- “NN distance > s” ⇒ none of the other $N-1$ points inside the disk of radius s

Nearest Neighbor (NN) Distance Between Nucleation Sites

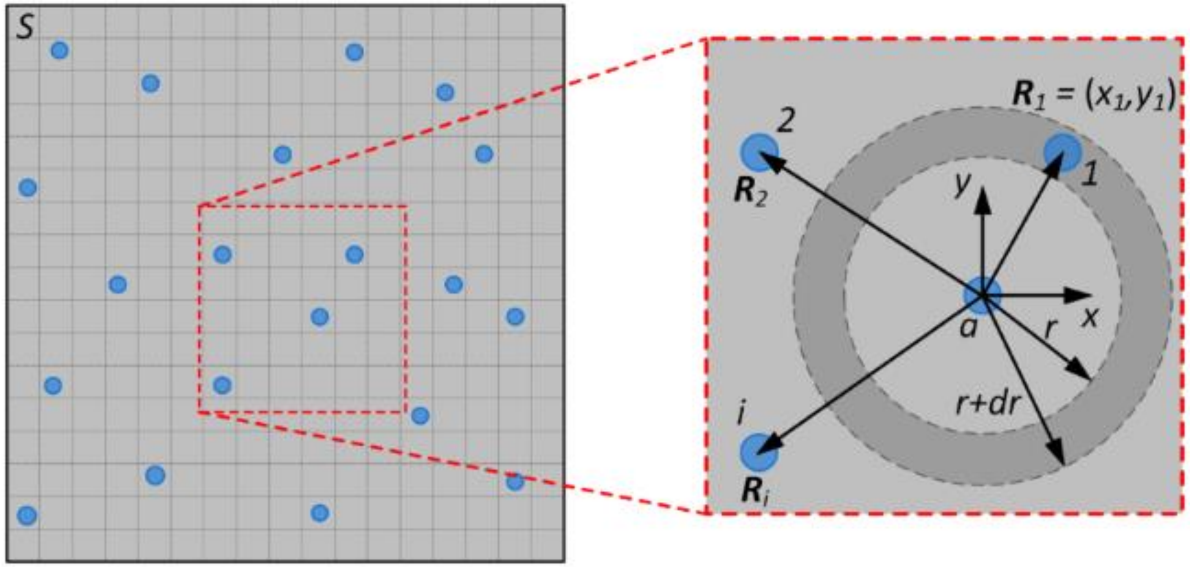

- Assuming the surface is sufficiently large (no edge effects)

$$\Pr(r > s) = \left(1 - \frac{\pi s^2}{A}\right)^{N-1} \Rightarrow \Pr(r \leq s) = 1 - \left(1 - \frac{\pi s^2}{A}\right)^{N-1}$$

Nearest Neighbor (NN) Distance Between Nucleation Sites

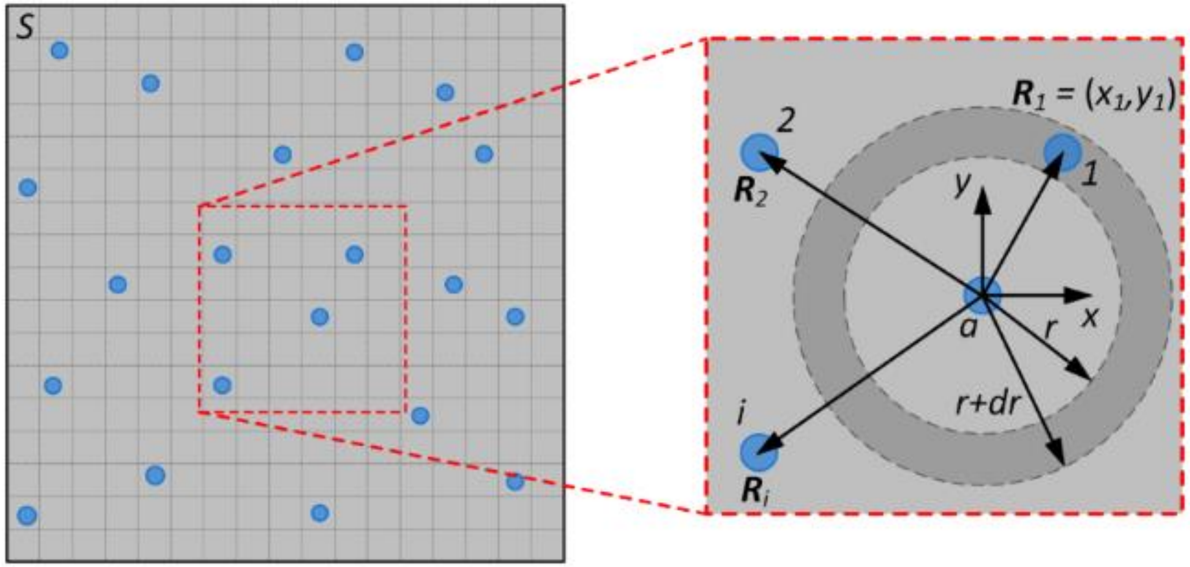

$$\Pr(r \leq s) = 1 - \left(1 - \frac{\pi s^2}{A}\right)^{N-1}$$

The probability distribution function for NN distance $f(s)$

$$f(s) = \frac{d}{ds}\left(\Pr(r \leq s)\right) = (N-1)\frac{2\pi s}{A}\left(1 - \frac{\pi s^2}{A}\right)^{N-2}$$

For $N \to \infty$ and $A \to \infty$

$$f(s) \approx \frac{2\pi N}{A} s \cdot \exp\left(-\frac{\pi N}{A} s^2\right)$$

Rayleigh distribution

Number of Isolated Bubbles

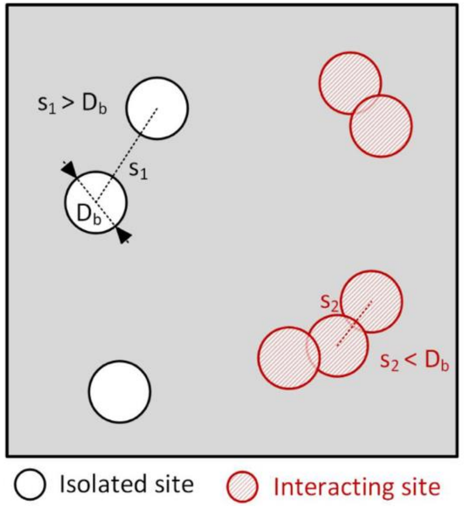

$$P_{iso} = P(s > D_b) = \int_{D_b}^{\infty} f(s)ds = \int_{D_b}^{\infty} \frac{2\pi N s}{A} e^{-\frac{\pi N s^2}{A}} ds = e^{-\frac{\pi N D_b^2}{A}}$$

$$N_{iso} = \sum_{N=1}^{\infty} N P_{iso} \mathrm{Po}(N, N_0) = \sum_{N=1}^{\infty} \frac{N_0^N}{(N-1)!} \exp\left(-N_0 - \frac{\pi N D_b^2}{A}\right)$$

CHF Criteria

$$\frac{\partial N_{iso}}{\partial T} = 0$$

$$\frac{\partial}{\partial T}\left[\sum_{N=1}^{\infty} \frac{N_0^N}{(N-1)!} \exp\left(-N_0 - \frac{\pi N D_b^2}{A}\right)\right] = 0$$

$$\Rightarrow n_0 \pi D_b^2 = 1$$

A unified relationship between the nucleation density at CHF and bubble diameter

Beyond Boiling

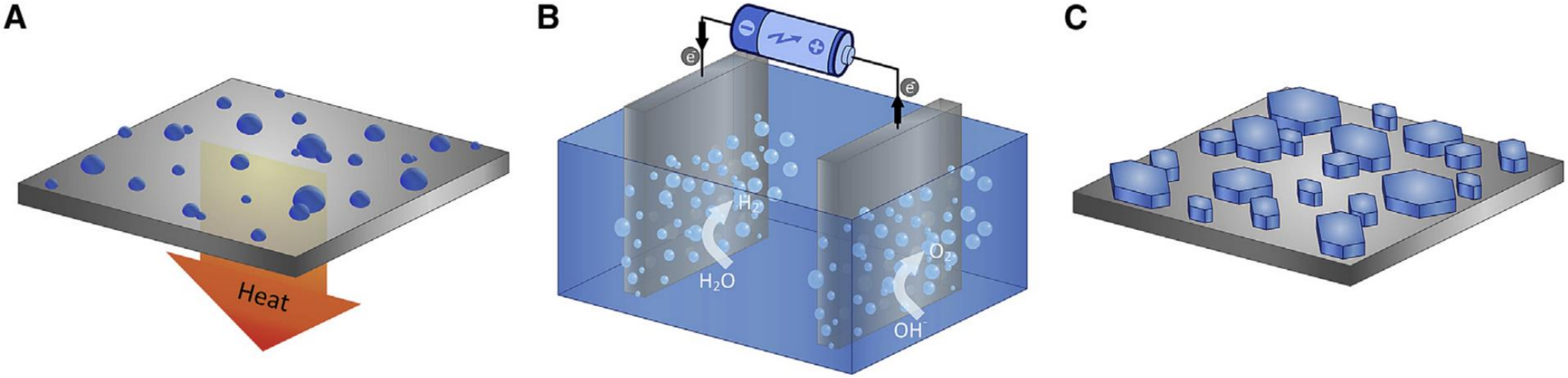

Condensation

Water splitting

Material growth

Zhang *et al.*, *Cell Reports Physical Science* 2020

Gas Evolving Reaction (GER)

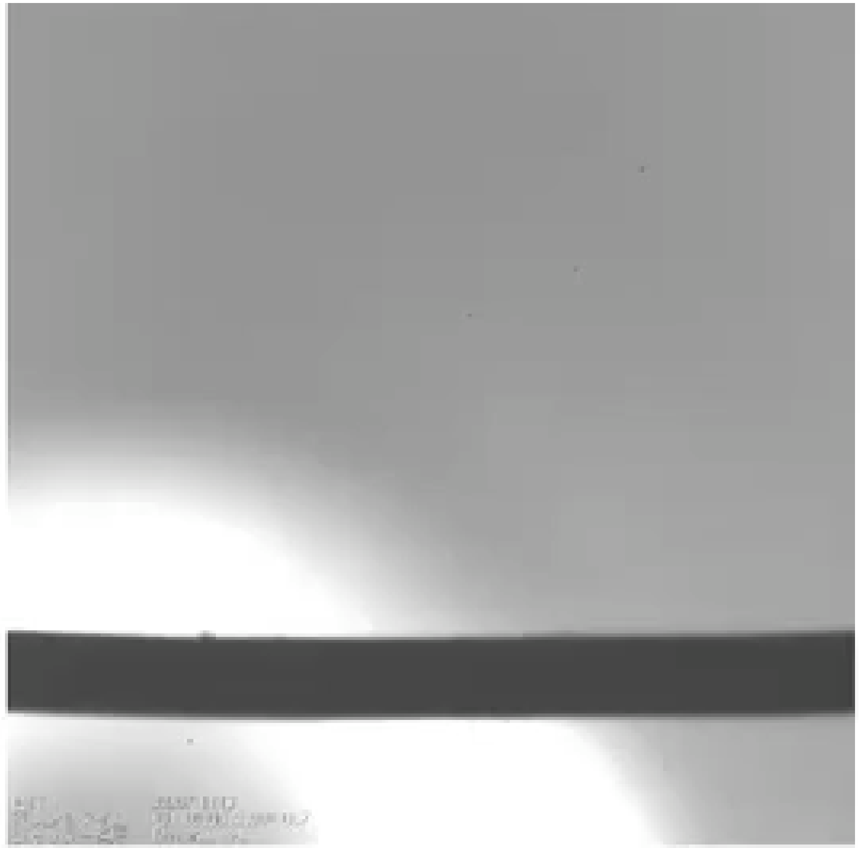

Industrial electrochemical processes that involves bubbles

Water splitting

Aluminum production

Sodium chlorate production

Chlorine and sodium hydroxide production

https://doi.org/10.1016/j.ijhydene.2022.01.166

Effect of Bubbles on Electrochemical Reactions

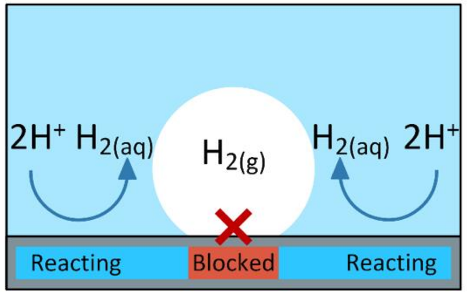

Blocking reaction area

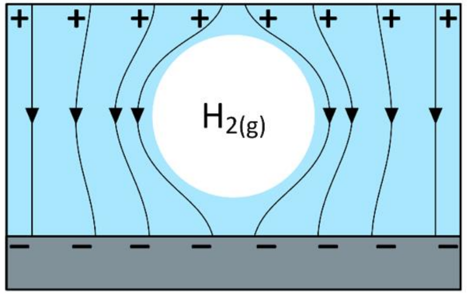

Additional resistance for ion transport

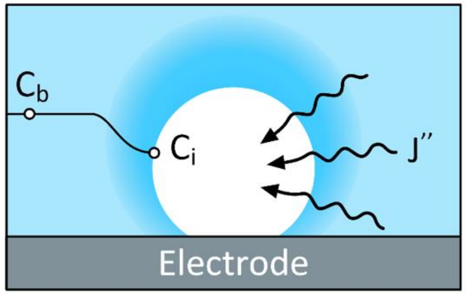

Additional diffusion resistance

Bubble-induced convection

Boiling and GER

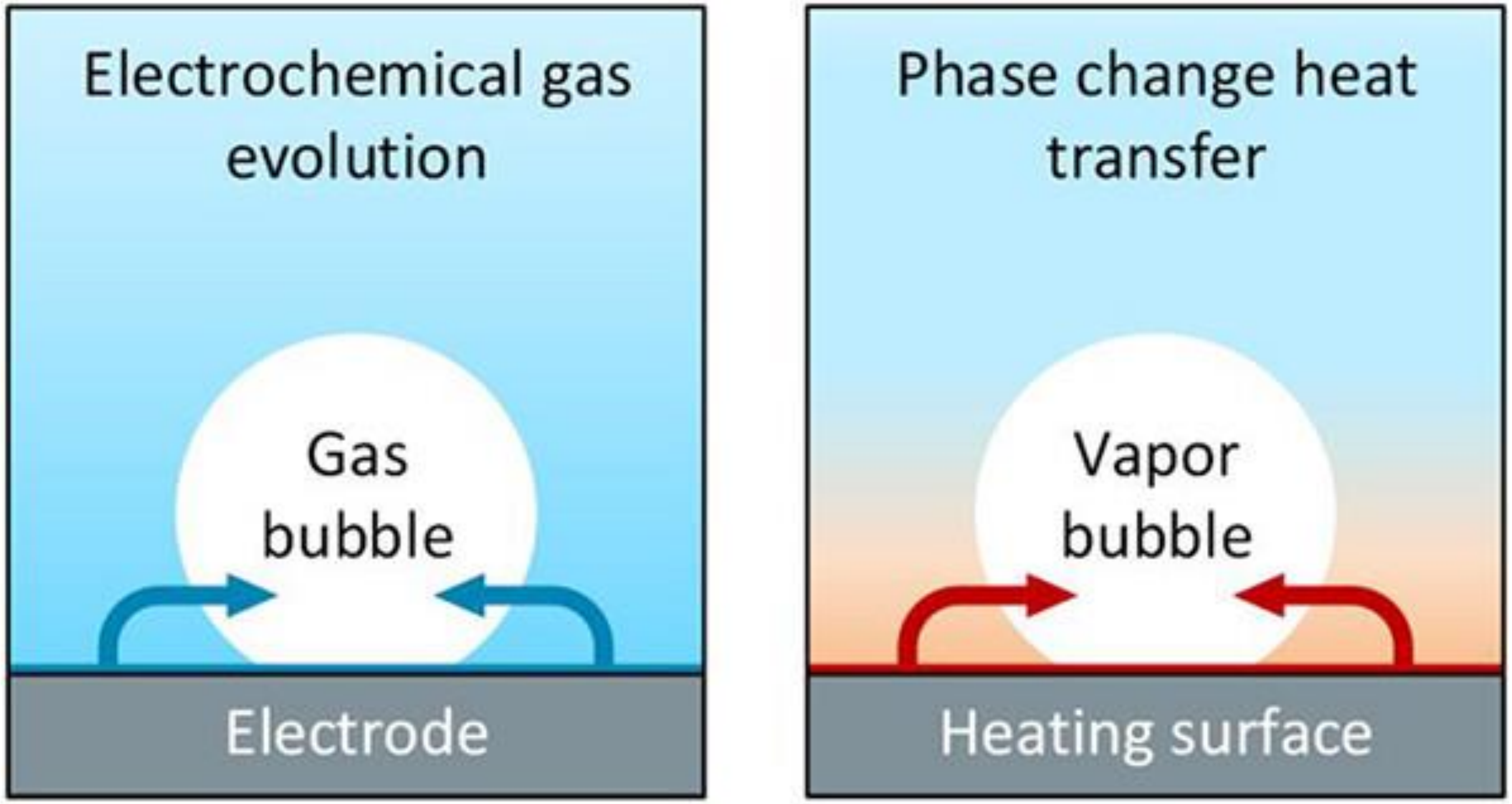

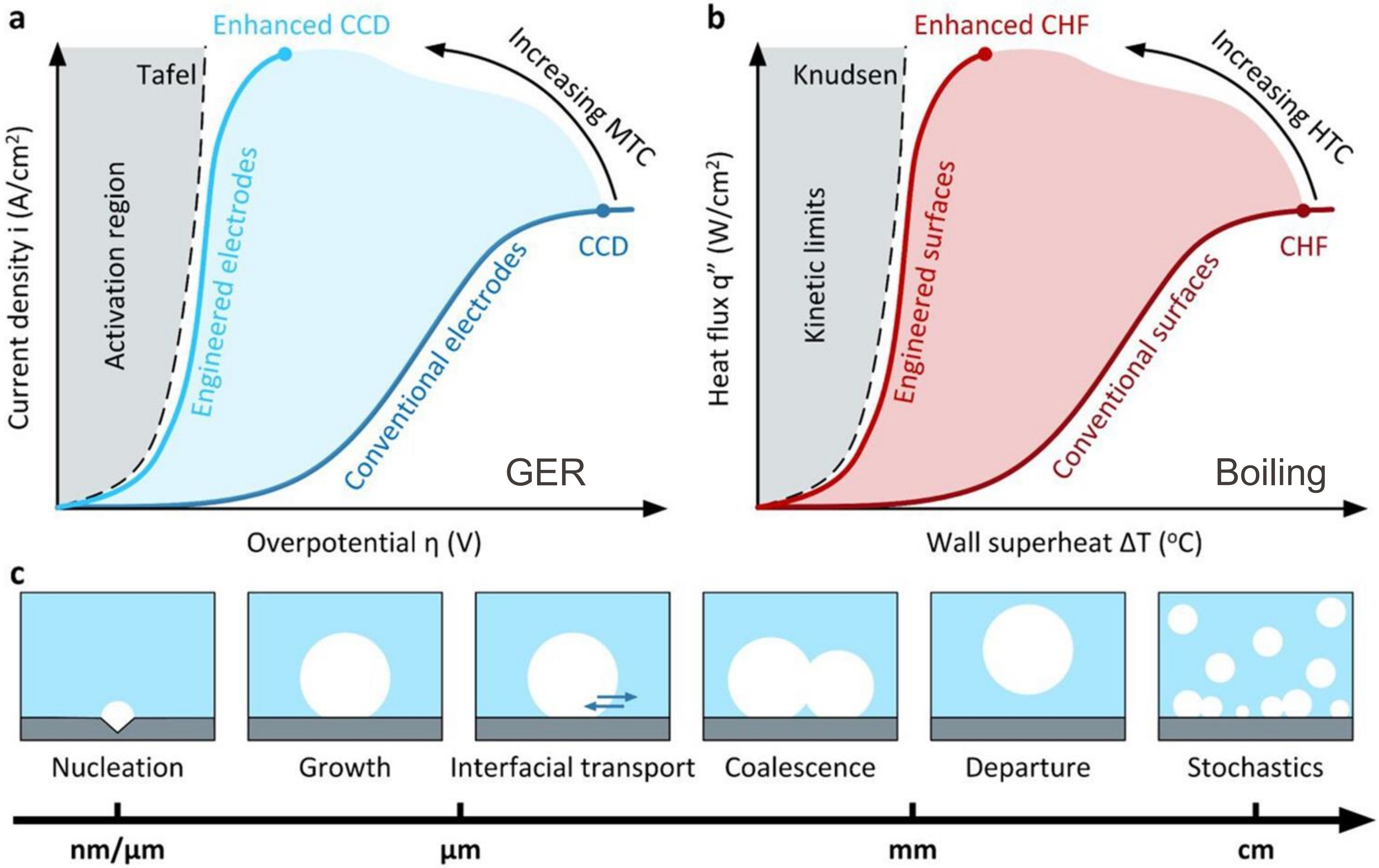

doi.org/10.1021/acs.chemrev.4c00157

Coalescence-Driven Bubble Departure

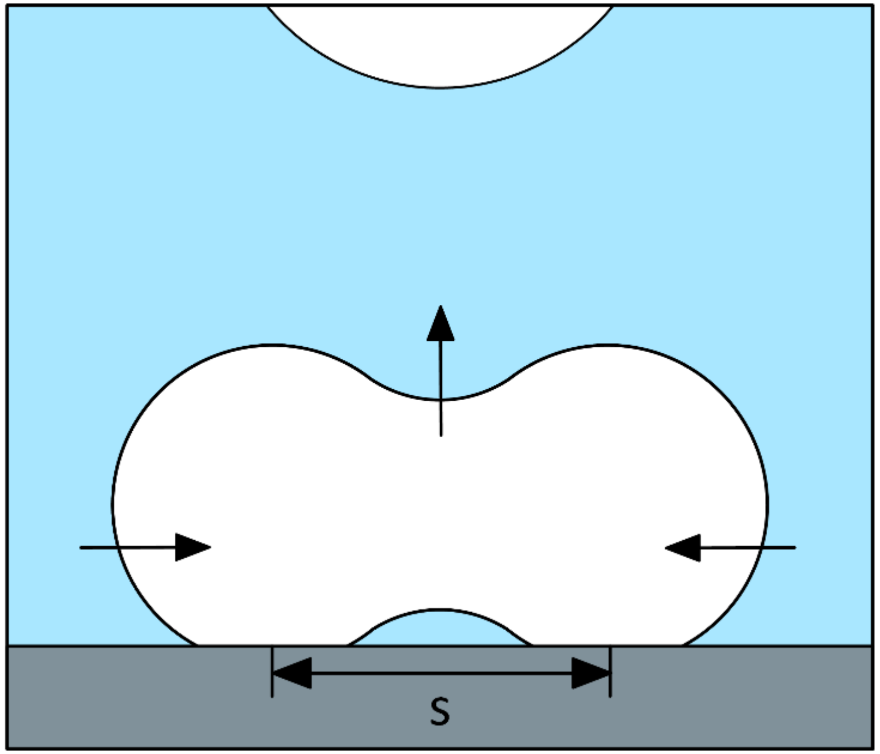

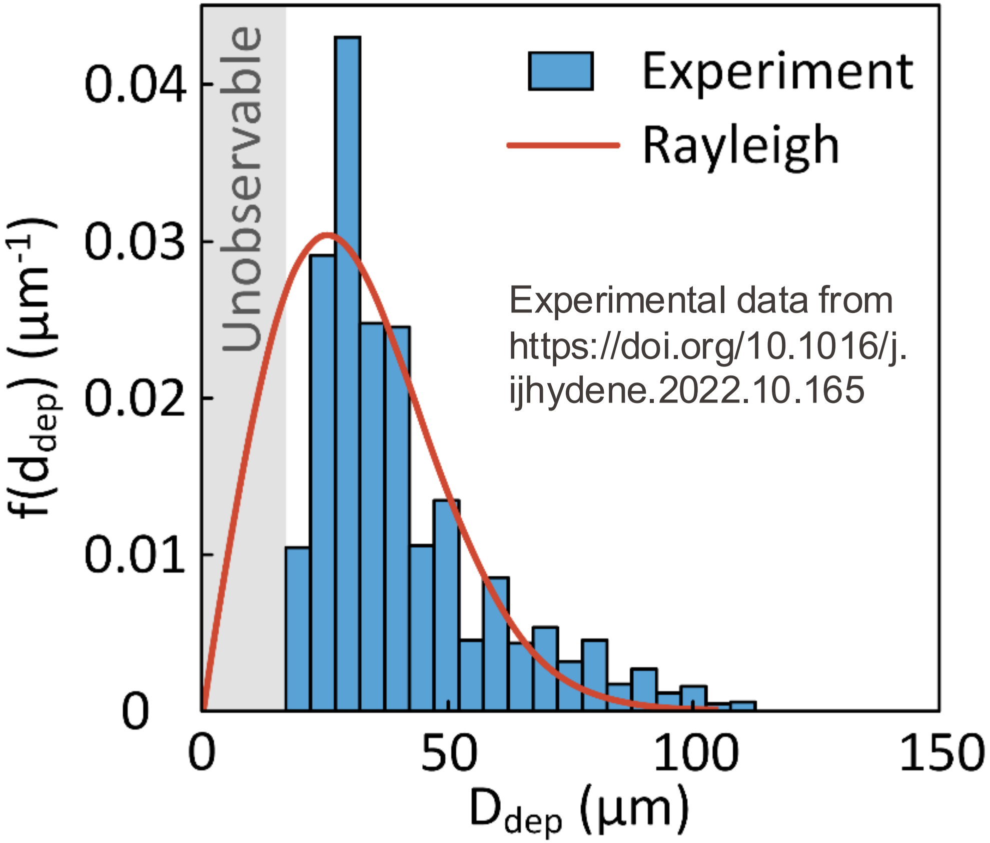

Experimental data from https://doi.org/10.1016/j.ijhydene.2022.10.165

- When two bubbles coalesce into one, surface area becomes smaller. Excess surface energy needs to be released.
- This may cause bubble to depart immediately after contacting its nearest neighbor